Laser and Particle Beams (2009), *27*, 681–687.

doi:10.1017/S0263034609990401

A composite phase conjugator based on Brillouin-enhanced four-wave mixing combining with stimulated Brillouin amplification

C.Y. ZHU, Z.W. LU, AND W.M. HE

Institute of Opto-electronics, Harbin Institute of Technology, Harbin, China

(RECEIVED 25 June 2009; ACCEPTED 7 September 2009)

Abstract

A novel composite optical phase conjugator that combines Brillouin-enhanced four-wave mixing (BEFWM) and stimulated Brillouin amplification (SBA) in a compact structure is reported. A phase-conjugate wave seed is generated by BEFWM process with characteristics such as fast response, high conjugate fidelity and stability, then it is magnified by SBA with high energy-conversion efficiency. As a result, advantages of BEFWM and SBS can be realized at the same time. This composite conjugator has potentials for high-peak and high-average power laser applications, especially for short pulse or steep leading-edge pulse laser systems. Feasibility of this BEFWM-SBA mechanism is verified in theoretical simulations and demo experiments.

Keywords: Brillouin-enhanced four-wave mixing; Composite phase conjugator; High-power laser; Optical phase conjugation; Stimulated Brillouin scattering

1. INTRODUCTION

Stimulated Brillouin scattering (SBS) optical phase conjugation (OPC), a technique with profound significance to high-power laser science, has been studied and made great efforts to application practically by researchers all over the world for decades (Zel'dovich *et al.*, 1972; Basov & Zubarev, 1979; Meister *et al.*, 2007; Ostermeyer *et al.*, 2008). In demand for large laser engineerings such as inertial confinement fusion and inertial fusion energy, works on SBS phase conjugator, SBS beam combiner, and so on, are being carried out by more and more research teams (Kong *et al.*, 2005, 2006, 2007, 2008, 2009; Kappe *et al.*, 2007; Hasi *et al.*, 2007, 2008; Wang *et al.*, 2007, 2009; Yoshida *et al.*, 2007). As well known, advantages of the SBS phase conjugator are high energy-conversion efficiency and simple structure. However, the acoustic wave, which plays a crucial role in SBS process, is developed from the noise in Brillouin medium (Boyd *et al.*, 1990), which makes the phase-conjugate wave instable in many situations. For instance, phase jumps or intensity modulations are frequently observed in experiments (Shahraam *et al.*, 1998; Yang *et al.*, 2001), and when the leading-edge of the laser pulse is shorter than or comparable with the phonon lifetime of the Brillouin medium, SBS phase-conjugate fidelity and its stability will deteriorate severely (Dane *et al.*, 1992), which keeps this technique far away from applications of short pulse such as fast ignition laser pulse. Besides, the Stokes wave competes with optical noise modes throughout its generation and amplification processes, leading to the existence of non-conjugate components of the output wave, that is to say, the phase-conjugate fidelity can never really achieve 100% (Zeldovich *et al.*, 1982). So far as it goes, problems mentioned above, whose root is the noise-origin characteristic of the acoustic wave, have become severe limiting factors for practical application of SBS phase conjugator.

There is another OPC technique, called Brillouin-enhanced four-wave mixing (BEFWM), which is also based on acousto-optic interaction, but different from SBS in acoustic origin mechanism in nature (Scott & Ridley, 1989). In BEFWM process, acoustic wave is driven by optical coherent beating patterns and built up instantaneously without acoustic-relaxation-time restriction of the medium. This non-noise process not only keeps OPC stable and transient-state-adaptable but also exhibits advantages as non-threshold and a 100% conjugate fidelity. In the past decades, researches on BEFWM mainly focused on the

Address correspondence and reprint requests to: Zhi Wei Lu, Institute of Opto-Electronics, Harbin Institute of Technology P.O. Box 30031, Harbin 150080, China. E-mail: zw_lu@sohu.com

conjugate-amplification of weak optical signals, and have gain many achievements (Andreev *et al.*, 1989; Lanzerotti *et al.*, 1996; Zhu *et al.*, 2007). However, when BEFWM operates with large incident signals as a high-power phase conjugator, its efficiency, i.e., total reflectivity, will be low because the energy of the conjugate wave comes from the reference wave instead of the signal wave itself (Zhu *et al.*, 2008).

In this paper, a composite phase conjugator scheme, in which mechanism of BEFWM and SBS are combined in a compact structure is reported. The BEFWM provides phase-conjugate wave seed with fast response, high quality and stability, which is then magnified by stimulated Brillouin amplification (SBA) with high energy-conversion efficiency. As a result, advantages of BEFWM and SBS can be realized at the same time. In the following sections, the theoretical model is set up, as well as numerical simulations, and demo experiments are carried out. Feasibility of the BEFWM-SBA phase conjugator is verified sufficiently.

2. THEORY

2.1. Physical Model

Physical model of the BEFWM-SBA composite phase conjugator is shown in Figure 1. E_1 and E_2, in Figure 1a, are counter-propagating reference waves, while E_2 has a relative Stokes-shift in frequency. The laser signal wave E_3, as the main laser wave whose power is much greater than the reference waves, intersects E_1 at a small angle, and its conjugate wave generated by the phase conjugator is termed as E_4. All the input waves should be linearly polarized, among which E_1 is in p-polarized-state, E_2 is in s-state, and let the polarized direction of E_3 be slanted slightly, so as to share its power in s-state for a little and most of them be contained in p-state.

In order to describe these polarization states more explicit, we add letters p and s to the wave notations in Figure 1b, and term the two polarized components of E_3 as E_{3p} and E_{3s} separately. The physical picture of interaction among these waves can be depicted as follows: when encounterring in the Brillouin medium, s-state E_{3s} and E_{2s} interfere with each other and drive the periodic density variations in the medium that travels from left to right at a velocity close to the velocity of sound in the medium, thus an acoustic wave ρ_{FWM} with frequency Ω is produced as a result. ρ_{FWM} acts as a moving Bragg-phase grating, once founded, it will scatter E_{1p} and generate the p-state Stokes-shifted wave E_{4p}, which is phase conjugated with the laser signal E_3. Then, as E_{4p} propagates opposite to the way of E_3, it will be Brillouin-amplified by E_{3p} which is also in the p polarized direction, and high efficiency power growth can be realized.

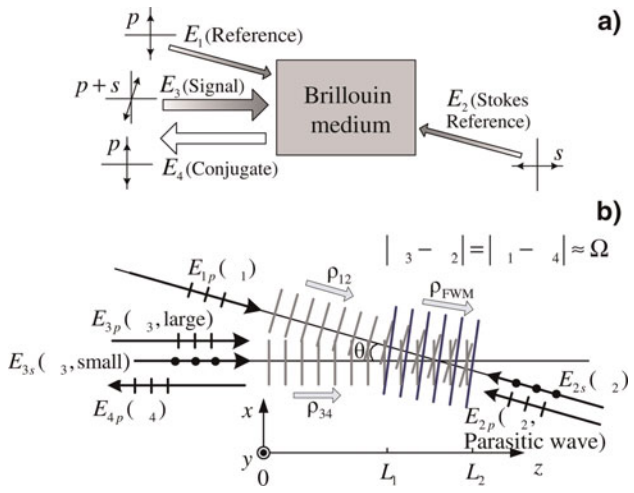

Fig. 1. Physical model of the composite-mechanism phase conjugator scheme.

There are two procedures existing in this scheme. At first, a phase conjugate wave seed is generated through Stokes-type polarization-decoupled BEFWM. Then, growth of the conjugate wave mainly depends on the SBA process. The former process provides characteristics for E_4 as high stability and fidelity, the later one ensures high conversion efficiency. In this way, advantages of BEFWM and SBS can be realized in the composite phase conjugator at the same time.

However, when ρ_{FWM} is built, waves in all polarized states will be scattered by it immediately. According to the propagating direction of ρ_{FWM}, the signal component E_{3p} might be Stokes-scattered by ρ_{FWM} and generate a Stokes-shifted wave E_{2p}, which is conjugated with E_{1p}. We call E_{2p} a parasitic wave. Here come two harmful effects from the parasitic wave. First, power in E_{3p} will be lost partly, resulting in decrease of the Brillouin amplification gain of E_{4p}. Second, E_{2p} will be Brillouin amplified by E_{1p} and therefore reduce the E_{1p} power that should be transported into E_{4p} through BEFWM process. So, how to ensure that E_{4p} have the dominance over E_{2p} during all the processes of generation and amplification is an important issue for this conjugator scheme.

2.2. Mathematical Model

In the following mathematical model, the acoustic waves of SBA in two different directions, i.e., E_{3p} *versus* E_{4p} and E_{1p} *versus* E_{2p}, are denoted as ρ_{34} and ρ_{12}, respectively, which propagate from left to right too. All of the six optical waves can be described by Maxwell's wave equations, and the three acoustic waves can be depicted by Navier-Stokes's energy transmission equation. Taking the interaction geometry into account as shown in Figure 1b, and based on the assumption of neglecting in the second derivations, the nonlinear coupled-equations describing all the processes mentioned above along the z direction can be written as

$$\left(\cos\theta\frac{\partial}{\partial z}+\frac{n}{c}\frac{\partial}{\partial t}\right)E_{1p}=ig_o\rho_{12}E_{2p}+ig_o\rho_{FWM}E_{4p}-\frac{\alpha}{2}E_{1p}, \quad (1)$$

$$\left(-\cos\theta\frac{\partial}{\partial z}+\frac{n}{c}\frac{\partial}{\partial t}\right)E_{2s}=ig_o\rho^*_{FWM}E_{3s}\exp(i\Delta kz)-\frac{\alpha}{2}E_{2s}, \quad (2)$$

https://doi.org/10.1017/S0263034609990401 Published online by Cambridge University Press

$$\left(-\cos\theta\frac{\partial}{\partial z}+\frac{n}{c}\frac{\partial}{\partial t}\right)E_{2p}=ig_o\rho_{12}^{*}E_{1p}+ig_o\rho_{FWM}^{*}E_{3p}\exp(i\Delta kz)-\frac{\alpha}{2}E_{2p}, \tag{3}$$

$$\left(\frac{\partial}{\partial z}+\frac{n}{c}\frac{\partial}{\partial t}\right)E_{3s}=ig_o\rho_{FWM}E_{2s}\exp(-i\Delta kz)-\frac{\alpha}{2}E_{3s}, \tag{4}$$

$$\left(\frac{\partial}{\partial z}+\frac{n}{c}\frac{\partial}{\partial t}\right)E_{3p}=ig_o\rho_{34}E_{4p}+ig_o\rho_{FWM}E_{2p}\exp(-i\Delta kz)-\frac{\alpha}{2}E_{3p}, \tag{5}$$

$$\left(-\frac{\partial}{\partial z}+\frac{n}{c}\frac{\partial}{\partial t}\right)E_{4p}=ig_o\rho_{34}^{*}E_{3p}+ig_o\rho_{FWM}^{*}E_{1p}-\frac{\alpha}{2}E_{4p}, \tag{6}$$

$$\left(\frac{\partial}{\partial t}+\frac{\Gamma_B}{2}+i\Delta\Omega\right)\rho_{FWM}=ig_a(\theta)[E_{3s}E_{2s}^{*}\exp(i\Delta kz)+E_{1p}E_{4p}^{*}\cos\theta+E_{3p}E_{2p}^{*}\cos\theta\exp(i\Delta kz)], \tag{7}$$

$$\left(\frac{\partial}{\partial t}+\frac{\Gamma_B}{2}\right)\rho_{12}=ig_aE_{1p}E_{2p}^{*}, \tag{8}$$

and

$$\left(\frac{\partial}{\partial t}+\frac{\Gamma_B}{2}\right)\rho_{34}=ig_aE_{3p}E_{4p}^{*}, \tag{9}$$

where E and ρ are amplitudes of optical and acoustic wave, respectively; c is light velocity in the vacuum; n denotes the refractive index; $g_a(\theta)$ is the acoustic coupling coefficient with the angle θ between the optical waves, and numerically equals to $g_a\cos^2(\theta/2)$ (Aschroeder *et al.*, 1989), in which g_a is the value for $\theta=0$; Γ_B is the Brillouin linewidth of the medium; $\Delta\Omega=\Omega(\cos(\theta/2)-1)$ and $\Delta k=(\Delta\bar{k})_z=n\Omega(\cos\theta-1)/c$ represent, respectively, the frequency detuning and the phase mismatch of acoustic waves in BEFWM; α is the optical absorption coefficient. Compared with the light velocity, the sound velocity is so small that the propagation terms have been neglected in the three acoustic waves, Eqs. (7–9).

According to Figure 1b, E_{1p}, E_{3p}, and E_{3s} are injected at $z=0$ while E_{2s} at $z=L_2$. E_{4p} and E_{2p} equal to zero at $z=L_2$ or when $t=0$. Intensities of other optical waves will be specified as demand. Interaction length of BEFWM is limited between L_1 and L_2, and where out of this range, the gain of BEFWM equals to zero. Brillouin amplifications exist in the entire space $0\sim L_2$ along the propagation directions of E_1 and E_3. So far, all the boundary and initial conditions of the equations are defined, and the numerical simulation can be carried out.

2.3. Simulation and Analysis

In the numerical simulation, the laser signal is chosen as 1.06-μm wavelength and 20-ns full width at half maximum Gaussian pulses. CS_2 is chosen as the Brillouin medium (Hasi *et al.*, 2005), whose $n=1.59$, SBS gain coefficient is 68 cm/GW, the phonon lifetime is 6.4 ns, and $\alpha=4\times10^{-3}\text{cm}^{-1}$. Besides, we set the parameters as: $L_1=35$ cm, $L_2=50$ cm, $\theta=10$ mrad, the peak intensity ratio of the reference waves is $|E_{1p}|^2:|E_{2s}|^2=I_{1p}:I_{2s}=2$, and the peak intensity ratio of the two polarization components in the signal E_3 is $|E_{3p}|^2:|E_{3s}|^2=I_{3p}:I_{3s}=20{:}1$.

As mentioned above, suppression of the parasitic wave E_{2p} is important. An effective method to realize it is to decrease I_{1p} comparing with I_{3p}, i.e., to decrease the pumping intensity in the SBA process of the parasitic wave E_{2p}, so as to decrease the energy extraction ratio for E_{2p} from E_{1p}. To do this, although the initial intensity of E_{4p} generated in BEFWM will be weaker, it can be amplified to become a considerable magnitude by the high-intensity pump wave E_{3p} in the following SBA process. In Figure 2a, the simulating input pulse waveforms of E_{1p}, E_{3p}, and the output waveforms of E_{4p} and E_{2p} are shown in the same intensity scale when the injected peak intensities $I_{3p}=50\ \text{MW/cm}^2$ and $I_{3p}=5\ \text{MW/cm}^2$. It is easy to demonstrate that the output E_{2p} is rather weak.

Another method helping to suppress the E_{2p} pulse is to set injecting temporal delay for E_3 relative to E_1 pulse, through which, when E_3 arrives in the BEFWM region and E_{2p} is generated, there is only a tail part of the E_{1p} pulse to provide energy transfering to E_{2p} in the SBA process, which is very limited in energy and actuation duration. Nevertheless, if only the conjugate wave seed E_{4p} is generated, even though its duration of generation is short and intensity is weak, it can be amplified during the whole subsequent signal pulse span with a high gain. In Figure 2b, it is set as $I_{1p}=5\ \text{MW/cm}^2$, $I_{1p}=50\ \text{MW/cm}^2$, and E_3 is delayed by 20 ns relative to E_1. It can be seen that peak intensity of the conjugate pulse E_{4p} is close to 50 MW/cm^2, while E_{2p} can almost be neglected.

Other parameter-contributions to the composite PC have been calculated numerically in our theoretical simulation work, and feasibility of this composite-mechanism scheme is verifed in the theory. Performance of the PC, such as reflectivity will be discussed in the next section.

3. EXPERIMENTS

3.1. Experimental Setup

The experimental setup is shown in Figure 3. The Nd:YLF single frequency TEM_{00} Q-switched laser, operating at 1-Hz repetition rate, can deliver about 120 mJ *p*-polarized-state pulses at 1053 nm in a 20-ns full width at half maximum quasi-Gaussian pulse shape. The beam diameter is about 4 mm. A $\lambda/2$ plate and polarizer P_1 are used to split the laser beam into E_1 wave, i.e., E_{1p}, and E_3 wave. After passing through the 4% sampling plate SP_1 and the polarizer P_4, E_{1p} enters the 80-cm-length composite cell filled with CS_2, i.e., Cell-1, and the forepart of E_{1p} pulse that transmitted throughout of Cell-1 generates backward Stokes wave in a short-focused-type SBS CS_2 cell, i.e., Cell-2, whose lens focus equals to 10 cm and distance from Cell-1 is about 70 cm. When passing backward through the $\lambda/4$ plate, the

https://doi.org/10.1017/S0263034609990401 Published online by Cambridge University Press

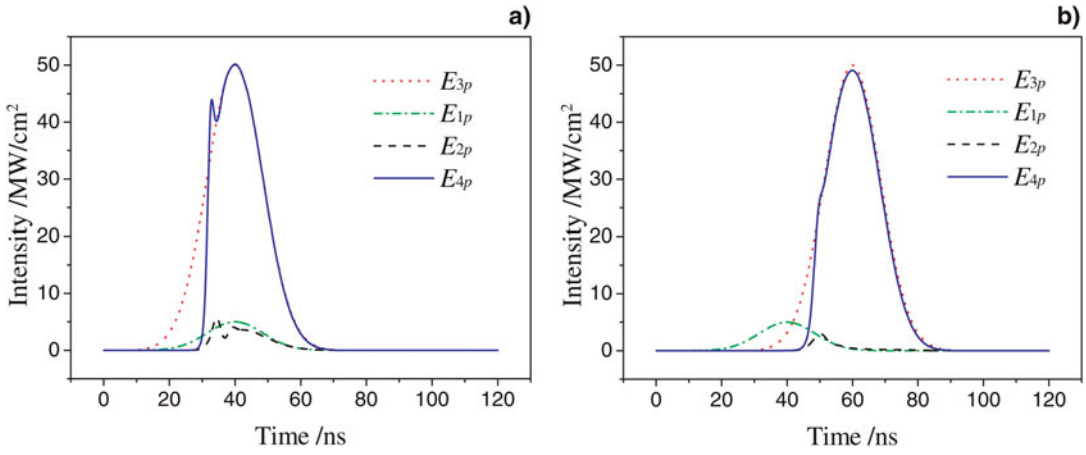

Fig. 2. Numerical simulation on the input and output waveforms of the conjugator when the incident peak power $I_{3P} = 50\ \mathrm{MW/cm^2}$, $I_{1P} = 5\ \mathrm{MW/cm^2}$, without signal delay (**a**), and with 20-ns signal delay (**b**).

Stokes wave is changed into *s*-polarized state, then enters into the back window of Cell-1, and acts as E_{2s}. The E_3 wave, which is reflected by the polarizer P_1 and then by P_2 turns into *p*-polarized state by a 45° rotor and a 45° Farady rotator, and penetrates through the polarizer P_3 entirely. Then it is adjusted by a $\lambda/2$ plate to contain a small *s*-state component with ratio of $I_{3p}/I_{3s} = 20$, and coupled by 20-ns delay mirrors $M_1 \sim M_6$ into Cell-1 where BEFWM-SBA process is built up. The angle between E_1 and E_3 is about 10 mrad. The penetrated part of E_3 is obstructed by a diaphragm set behind Cell-1. The conjugate wave E_{4p} generated in Cell-1 propagates backward along the way of E_3, and finaly penetrates P_2 to become the output wave. The residual E_{2s} and the parasite wave E_{2p} will propagate backward along the way of E_1. E_{2s} will be reflected off by the polarizer P_4, and E_{2p} can be blocked by the isolator.

In the experiments, we recorded the injection E_{1p} and the output of E_{2p} on the two sides of SP_1, and recorded E_3 and E_{4p} on SP_2 simultaneously. In order to simulate high-flux laser system, a long focus lens with $f = 300$ cm is inserted in the path of E_3 to increase the signal intensity to a certian extent in the BEFWM-SBA region, while the focus of the 300-cm lens is located out of the Cell-1 in order to avoid self-excitational SBS of E_3.

3.2. Results and Discussion

Pulsed waveforms and near-field intensity patterns of the input signal E_3 and the output conjugate wave E_4 measured in experiments are shown in Figure 4. A little step, which is usually observed in the Brillouin amplification process, is shown at the root of E_4 waveform. Consistency of the in and out beam cross-sectional patterns is achieved well.

In order to research the performance of the composite phase conjugator with different laser signal power, in the experiments, we fixed the incident E_1 at 8 mJ/pulse, and varied E_3 from 6 mJ/pulse to about 82 mJ/pulse gradually by changing the applied voltages charged on the Xe-lamps of the Nd:YLF laser. It is shown that the output E_4 increases from about 3 mJ/pulse to about 61 mJ/pulse, while the parasitic E_{2p} is kept in a range between about 3 mJ/pulse and 6 mJ/pulse, as shown in Figure 5.

Reflectivity *R* of the composite phase conjugator is defined as energy ratio of E_4 and E_3 pulses, i.e., $R = E_4/E_3$, which have been measured synchronously using the two same calorimeters at both sides of the sampling plate SP_2. For each measuring point, we recorded pulse energies continuously for 60 shots, and analyzed the mean value of *R* and its shot-to-shot fluctuations. In the discussion about, the

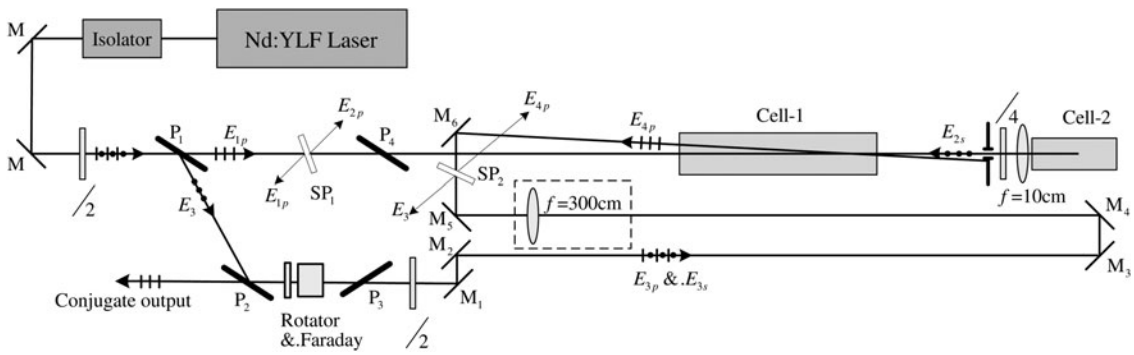

Fig. 3. Experimental setup of the BEFWM-SBA phase conjugator in demo-version.

https://doi.org/10.1017/S0263034609990401 Published online by Cambridge University Press

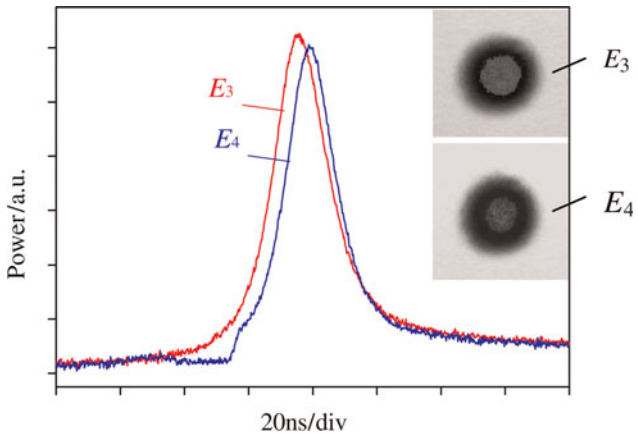

Fig. 4. (Color online) Pulsed waveforms and near-field intensity patterns of the input signal wave E_3 and the output conjugate wave E_4.

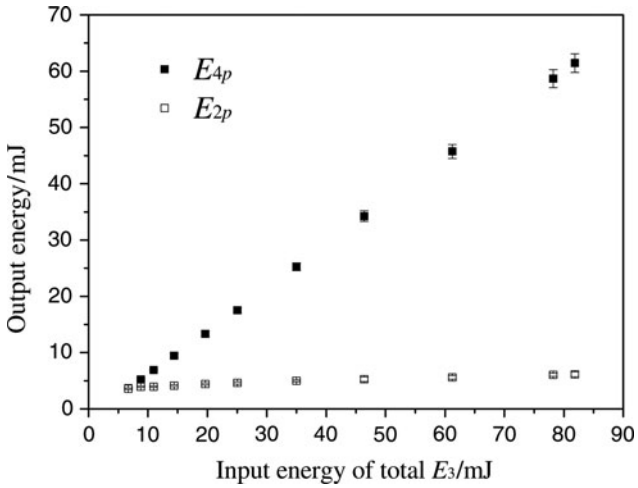

Fig. 5. Output pulse energies of E_4 and E_{2P} with different incident laser signal E_3.

stability of the conjugator, fluctuations of the laser itself should be taken into account, because variations in the signal can induce the change of R correspondingly. We note the relative instability of R with the symbol β, and calculate it by

$$\beta = \frac{\Delta R}{\bar{R}} = \frac{1}{\bar{R}}\left(\frac{\bar{E}_4}{\bar{E}_3}\Delta E_4 - \frac{\bar{E}_4}{\bar{E}_3^2}\Delta E_3\right),$$

where the symbol with bar on the head is the mean value at a certain measuring point, and Δ denotes the standard deviation, i.e., root mean square. Figure 6a shows the experimental results of R which is as a function of E_3. The increase of E_3 induced the growth of R from 55% to a saturation value about 75%. β is shown in Figure 6b. It is seen that β is almost fixed within the range close to or below 1% during the whole variation of E_3 and at any R values, which demonstrates a very good stability.

In Figure 6a, the theoretical result is shown as a solid line. Although the tendency of which is in accordance with the experiments, it is seen obviously that the deviation occurs when E_3 is larger. In our analysis, it is attributed to incomplete polarization control for the injecting optical waves.

Far-field divergence angles of the output conjugate wave E_4 is recorded by an array camera, the result is shown in Figure 7. When the signal increases, the mean value of the divergence angles of E_4 is about 0.451 mrad, which is close to the signal divergence 0.434 mrad. In addition, the fluctuation of the output divergence angles is below 5% in the whole experimental signal range.

4. CONCLUSIONS

A novel BEFWM-SBA composite phase conjugator can be realized by polarization control in a compact interaction region, in which generation and amplification of the phase

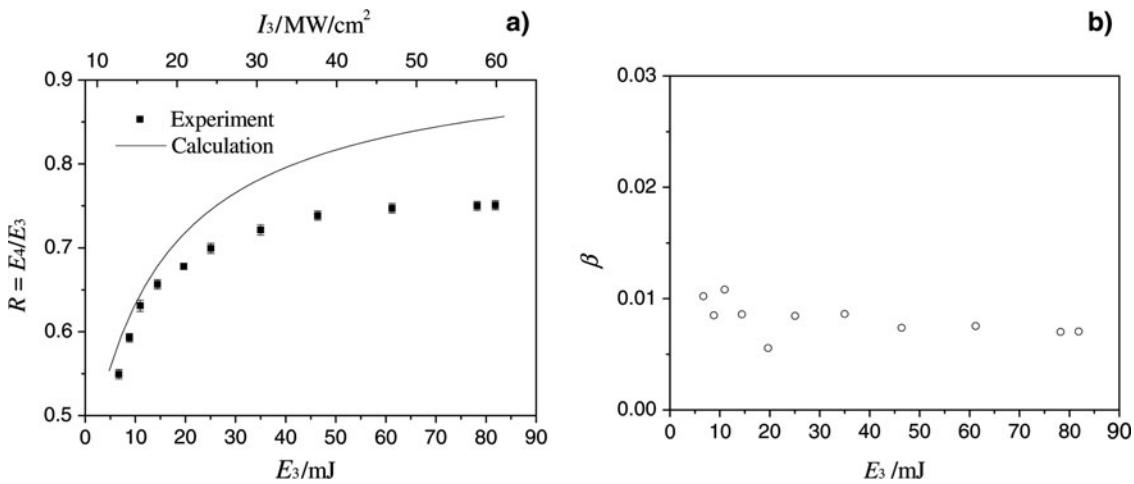

Fig. 6. Reflectivity R **(a)** and its relative instability β **(b)** with different incident laser signal E_3.

https://doi.org/10.1017/S0263034609990401 Published online by Cambridge University Press

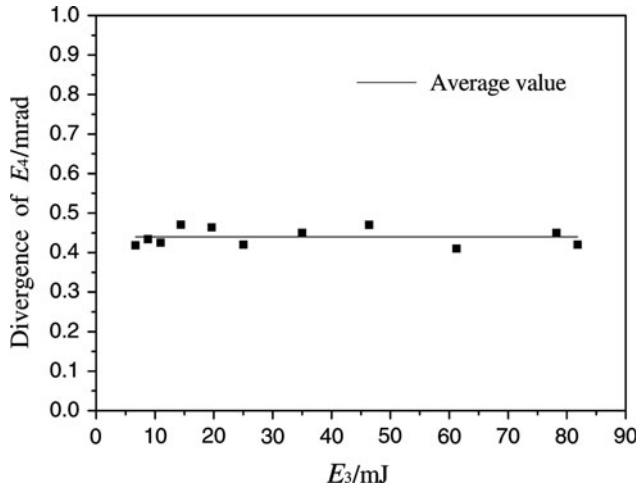

Fig. 7. Far-field divergence angles of the output conjugate wave E_4 with different incident laser signal E_3.

conjugate wave operates in BEFWM and SBA process, respectively. In this way, the advantages coming from non-noise origin of the acoustic wave and high-efficiency coupling can be achieved simultaneously very well, such as rapid response, high conjugate fidelity, high stability, and high efficiency.

Feasibility of this BEFWM-SBA mechanism is verified by the theoretical simulations and the experiments. Because almost all of the parameters are required adjustable in the demo-version experimental layout, it is seen rather complex in the structure, and a simplified version should be employed in the practical applications. For the experimental results in this paper, it is estimated that the incomplete control of the polarization states is the prime reason resulting in deviations of the experimental results from that of the theory. Besides, the output performance, such as a conjugation fidelity, which can be indicated by the far-field divergence angle, could be influenced by so many optical elements in the experimental setup.

Significant potential performance characteristics of the composite conjugator which will be very interesting are worth to be verified and studied in the following work. For instance, the transient-state adaptabitility supported by non-noise origin of the acoustic wave, the high repeat rate laser pulses, and the high-power laser-load adaptabitility because of the non-focus structure of the composite interaction region, and so on.

ACKNOWLEDGEMENTS

This work is supported by the National Natural Science Foundation of China (Grant No. 60878005), the National High Technology Development Program of China and the Program of Excellent Team in Harbin Institute of Technology. One of the authors, Cheng Yu Zhu, wishes to thank Professor Hong Jin Kong (Department of Physics, Korea Advanced Institute of Science and Technology) for his help in preparation of this paper.

REFERENCES

Andreev, N.F., Bespalov, V.I. & Dvoretsky, M.A. (1989). Phase conjugation of single photons. *IEEE J. Q.E.* **25**, 346–350.

Aschroeder, W., Damzen, M.J. & Hutchinson, M.H.R. (1989). Polarization-decoupled brillouin-enhanced four-wave mixing. *IEEE J. Q. E.* **25**, 460–469.

Basov, N. & Zubarev, I. (1979). Powerful laser systems with phase conjugation by SMBS mirror. *Appl. Phys.* **20**, 261–264.

Boyd, R.W., Rzazewski, K. & Narum, P. (1990). Noise initiation of stimulated Brillouin scattering. *Phys. Rev. A.* **42**, 5514–5521.

Dane, C.B., Neuman, W.A. & Hackel, L.A. (1992). Pulse-shape dependence of stimulated-Brillouin-scattering phase-conjugation fidelity for high input energies. *Opt. Lett.* **17**, 1271–1273.

Hasi, W.L.J., Gong, S., Lu, Z.W., Lin, D.Y., He, W.M. & Fan, R.Q. (2008). Generation of flat-top waveform in the time domain based on stimulated Brillouin scattering using medium with short phonon lifetime. *Laser Part. Beams* **26**, 511–516.

Hasi, W.L.J., Lu, Z.W., Li, Q. & He, W.M. (2007). Research on the enhancement of power-load of two-cell SBS system by choosing different media or mixture medium. *Laser Part. Beams* **25**, 207–210.

Hasi, W.L.J., Lu, Z.W., He, W.M. & Wang, S.Y. (2005). Study on Brillouin amplification in different liquid media. *Acta Phys. Sin. (in Chinese)* **54**, 742–748.

Kappe, P., Strasser, A & Ostermeyer, M. (2007). Investigation of the impact of SBS-parameters and loss modulation on the mode locking of an SBS-laser oscillator. *Laser Part. Beams* **25**, 107–116.

Kong, H.J., Lee, S.K. & Lee, D.W. (2005). Highly repetitive high energy/power beam combination laser: IFE laser driver using independent phase control of stimulated Brillouin scattering phase conjugate mirrors and pre-pulse technique. *Laser Part. Beams* **23**, 107–111.

Kong, H.J., Shin, J.S., Yoon, J.W. & Beak, D.H. (2009). Phase stabilization of the amplitude dividing four-beam combined laser system using stimulated Brillouin scattering phase conjugate mirrors, *Laser Part. Beams* **27**, 179–184.

Kong, H.J., Yoon, J.W., Beak, D.H., Shin, J.S., Lee, S.K. & Lee, D.W. (2007). Laser fusion driver using stimulated Brillouin scattering phase conjugate mirrors by a self-density modulation. *Laser Part. Beams* **25**, 225–238.

Kong, H.J., Yoon, J.W., Shin, J.S. & Beak, D.H. (2008). Long-term stabilized two-beam combination laser amplifier with stimulated Brillouin scattering mirrors. *Appl. Phys. Lett.* **92**, 021120.

Kong, H.J., Yoon, J.W., Shin, J.S., Beak, D.H. & Lee, B.J. (2006). Long term stabilization of the beam combination laser with a phase controlled stimulated Brillouin scattering phase conjugation mirrors for the laser fusion driver. *Laser Part. Beams* **24**, 519–523.

Lanzerotti, M.Y., Schirmer, R.W. & Gaeta, A.L. (1996). Phase conjugation of weak continuous-wave optical signals. *Phys. Rev. Lett.* **77**, 2202–2205.

Meister, S., Riesbeck, T. & Eichler, H.J. (2007). Glass fibers for stimulated Brillouin scattering and phase conjugation. *Laser Part. Beams* **25**, 15–21.

Ostermeyer, M., Kong, H.J., *et al.* (2008). Trends in stimulated Brillouin scattering and optical phase conjugation. *Laser Part. Beams* **26**, 297–362.

Scott, A.M. & Ridley, K.D. (1989). A review of Brillouin-enhanced four-wave mixing. *IEEE J. Q.E.* **25**, 438–459.

Shahraam, A., Vladimyros, D. & Jesper, M. (1998). Nature of intensity and phase modulations in stimulated Brillouin scattering. *Phys. Rev. A*. **57**, 3961–3971.

Wang, S.Y., Lu, Z.W., Lin, D.Y., Ding, L. & Jiang, D.B. (2007). Investigation of serial coherent laser beam combination based on Brillouin amplification. *Laser Part. Beams* **25**, 79–83.

Wang, Y.L., Lu, Z.W., He, W.M., Zheng, Z.X. & Zhao, Y.H. (2009). A new measurement of stimulated Brillouin scattering phase conjugation fidelity for high pump energies, *Laser Part. Beams* **27**, 297–302.

Yang, A.L., Yang, J.G., Ding, L., Li, M.Z., Zhang, X.M. & Mang, Y.Z. (2001). Phase Jump in the Process of Stimulated Brillouin Scattering. *Chinese J. Lasers*. **28**, 732–734.

Yoshida, H., Fujita, H., Nakatsuka, M., Ueda, T. & Fujinoki, A. (2007). Temporal compression by stimulated Brillouin scattering of Q-switched pulse with fused-quartz and fused-silica glass from 1064 nm to 266 nm wavelength.

Zel'dovich, B.Ya., Pilipetskii, N.F. & Shkunov, V.V. (1982). Phase conjugation in stimulated scattering. *Sov. Phys. Usp*. **25**, 713–737.

Zel'dovich, B.Ya., Popovichev, V.I., Ragul'skii, V.V. & Faizyllov, F.S. (1972). Connection between the wave fronts of the reflected and exciting light in stimulated Mandel'shtam- Brillouin scattering. *Soviet Phys. JETP lett*. **15**, 109.

Zhu, C.Y., Lu, Z.W., He, W.M., Ba, D.X., Wang, Y., Gao, W. & Dong, Y.K. (2007). Theoretical study on temporal behavior of Brillouin-enhanced four-wave mixing. *Acta Phys. Sin. (in Chinese)* **56**, 229–235.

Zhu, C.Y., Lu, Z.W., He, W.M., Guan, J. & Xu, X.C. (2008). Brillouin-enhanced four-wave mixing phase conjugation mirror with large signals. *Chinese J. Lasers. (in Chinese)* **35**, 845–848.

https://doi.org/10.1017/S0263034609990401 Published online by Cambridge University Press